

# Wigner representation for polarization-momentum hyperentanglement generated in parametric down conversion, and its application to complete Bell-state measurement

A. Casado<sup>1</sup>, S. Guerra<sup>2</sup>, and J. Plácido<sup>3</sup>.

<sup>1</sup> Departamento de Física Aplicada III, Escuela Técnica Superior de  
Ingeniería,  
Universidad de Sevilla, 41092 Sevilla, Spain.

Electronic address: acasado@us.es

<sup>2</sup> Centro Asociado de la Universidad Nacional de Educación a Distancia de  
Las Palmas de Gran Canaria,  
35004 Las Palmas de Gran Canaria, Spain.

<sup>3</sup>Departamento de Física, Universidad de Las Palmas de Gran Canaria,  
35017 Las Palmas de Gran Canaria, Spain.

PACS: 42.50.-p, 03.67.-a, 03.65.Sq, 03.67.Dd

## Abstract

We apply the Wigner function formalism to the study of two-photon polarization-momentum hyperentanglement generated in parametric down conversion. It is shown that the consideration of a higher number of degrees of freedom is directly related to the extraction of additional uncorrelated sets of zeropoint modes at the source. We present a general expression for the description of the quantum correlations corresponding to the sixteen Bell-like states, in terms of four beams whose amplitudes are correlated through the stochastic properties of the zeropoint field. Experiments on complete Bell-state measurement and quantum dense coding are analyzed, emphasizing the role of the vacuum field: it carries the quantum information which is extracted at the source, and also introduces some fundamental noise at the idle channels of the analyzers. These two features of the zeropoint field are a common denominator in optical experiments on quantum information.

Keywords: Entanglement, Bell-state analysis, parametric down conversion, Wigner representation, zeropoint field.

# 1 INTRODUCTION

In the last two decades, parametric down-conversion (PDC) assumed an important role for the practical implementation of the quantum theory of information, such as quantum cryptography [1], quantum dense coding [2] and teleportation [3]. The use of PDC as a source of entanglement involves the necessity of performing a complete Bell-state measurement (BSM), which is required in many quantum communication schemes. In this context, entangled photon pairs produced in PDC have been used for experiments on a partial Bell-state measurement [4], in which entanglement involves only one degree of freedom, and a complete Bell-state measurement, in which hyperentanglement (entanglement between two or more degrees of freedom) takes part [5]. More recently, these states have been used as an essential part of cluster states [6] of great value in the field of quantum computing [7].

The use of enlarged Hilbert spaces opened the door for a complete BSM using linear optics and single photon detectors, first by considering that one of the degrees of freedom was in a fixed quantum state [8], and encoding the information in the other degree of freedom. Further studies about the actual limits for BSM in these enlarged spaces have shown that, for two photons hyperentangled in  $n$  degrees of freedom, the number of mutually distinguishable sets of Bell states is bounded above by  $2^{n+1}$  [9]. More recently, it has been shown that at most  $2^{n+1} - 1$  classes out of  $4^n$  hyper-Bell states can be distinguished with one copy of the input state, and that a complete distinguishability is possible with two copies [10].

On the other hand, it is well known that the Wigner representation of quantum optics provides an alternative to the standard Hilbert space formalism for the study of quantum information and for its practical implementation with PDC. In the WRHP (Wigner representation within the Heisenberg picture) the generation and propagation of light is treated as in classical optics by taking into account the zeropoint field (ZPF) entering the crystal and the different optical devices placed between the source and the detectors. Finally, the vacuum fluctuations of the electromagnetic field are subtracted at the detectors [11, 12]. Hence, we can state that the peculiarities of the quantum world with respect to the image that classical physics offers are represented, in this context, by (i) the existence of a stochastic zeropoint field whose amplitudes are distributed according to a positive Wigner function, and (ii) the way in which the signal is separated from the zeropoint background in the detection process. These two features give rise to the typical

counterintuitive results within the quantum domain.

In essence, manipulating entanglement is a common denominator in the different manifestations of quantum communication. In the WRHP, two-photon polarization entanglement is represented by two stochastic light beams, whose correlation properties arise from the coupling between two zeropoint beams (each containing two sets of uncorrelated zeropoint modes) and the laser beam at the crystal [12], following the classical Maxwell equations [13, 14]. On the other hand, manipulating entanglement involves the change in the correlation properties of the light beams when they are going through the different optical devices, and this is related to the way in which the vacuum modes are redistributed at the field amplitudes. The description of two-qubit polarization entanglement for the four EPR states that can be generated via the process of PDC was made in [15] along with the application of the formalism to experiments on quantum cryptography. More recently, in [16] partial Bell-state analysis was studied, and the fermionic behaviour of two photons described by the singlet state when they reach a balanced beam-splitter was explained using purely wave-mechanical arguments based on the Wigner representation. These works emphasised the role of the zeropoint field in the generation and propagation of light in experimental implementations of quantum communication, including the existence of a relevant ZPF noise entering the idle channels of the analysers.

The standard Hilbert-space formulation of quantum optics considers vacuum fluctuations in an implicit way, through the Heisenberg principle and the use of normal ordering for the calculation of photodetection probabilities. In contrast, the Wigner function offers the possibility of stating specifically which is the role of vacuum fluctuations in the generation and measurement of quantum information, in quantum optical information processing using PDC. In this way, the motivation for this paper and further works comes from the following questions: What is the relationship between enlarging the Hilbert space and the zeropoint field activated at the source? Which is the role of the zeropoint at the different stages of a BSM experiment? Which is the relationship between the zeropoint modes entering the source, the ones that are activated at the idle channels of the analyzers, and the maximal information that can be generated in each experiment?

Thus there is considerable motivation for the application of the Wigner approach to the description of hyperentanglement generated using PDC, and the study of complete Bell-state analysis, in order to study the role of the zeropoint field in this area. In this paper we shall study a complete BSM

using polarization-momentum hyperentanglement generated in PDC, where one of the degrees of freedom is in a fixed quantum state, following the experimental setups of reference [8].

The paper is organised as follows: In Section 2 we shall describe two-photon polarization-momentum hyperentanglement generated in PDC, by means of four correlated light beams. This description involves the consideration of eight uncorrelated sets of vacuum modes, distributed in four ZPF entering beams at the source. We shall obtain a compact expression for the description of the sixteen Bell base states in the WRHP, in terms of six parameters. In Section 3 we will apply this formalism to study the experiments proposed in reference [8] in which one of the degrees of freedom is in a fixed quantum state. We will put the emphasis on the role of the zeropoint field at the different steps of each experiment, in order to make clear its relevance. Finally, in Section 4 we shall present the main conclusions of this work, and sketch further steps of future research.

## 2 POLARIZATION-MOMENTUM HYPER-ENTANGLEMENT IN THE WRHP

Let us start by considering the following situation: a type-I two-crystal source is pumped by a laser beam. In this source, the first (second) crystal emits pairs of horizontal (vertical) polarized photons in superimposed emission cones. Because the photons are emitted on opposite sides of the cone, two sets of conjugated beams,  $(a_1, b_2)$  and  $(a_2, b_1)$ , which are represented by wave vectors  $\mathbf{k}_{a_i}, \mathbf{k}_{b_i}$  ( $i = 1, 2$ ), can be selected [17]. If the coherence volume of the laser contains the two-crystal interaction region the quantum state corresponding to a photon pair, represented by the subscripts “1” and “2”, is usually expressed, in a particle-like description, as:

$$|\Phi^+\rangle \otimes |\psi^+\rangle = \frac{1}{\sqrt{2}}[|H\rangle_1|H\rangle_2 + |V\rangle_1|V\rangle_2] \otimes \frac{1}{\sqrt{2}}[|a\rangle_1|b\rangle_2 + |b\rangle_1|a\rangle_2]. \quad (1)$$

The state given by (1) is one of the sixteen base states corresponding to the two-photon hyperentanglement on polarization and momentum degrees of freedom [8]:

$$|\Psi^\pm\rangle \otimes |\psi^\pm\rangle = \frac{1}{\sqrt{2}} [|H\rangle_1 |V\rangle_2 \pm |V\rangle_1 |H\rangle_2] \otimes \frac{1}{\sqrt{2}} [|a\rangle_1 |b\rangle_2 \pm |b\rangle_1 |a\rangle_2], \quad (2)$$

$$|\Psi^\pm\rangle \otimes |\phi^\pm\rangle = \frac{1}{\sqrt{2}} [|H\rangle_1 |V\rangle_2 \pm |V\rangle_1 |H\rangle_2] \otimes \frac{1}{\sqrt{2}} [|a\rangle_1 |a\rangle_2 \pm |b\rangle_1 |b\rangle_2], \quad (3)$$

$$|\Phi^\pm\rangle \otimes |\psi^\pm\rangle = \frac{1}{\sqrt{2}} [|H\rangle_1 |H\rangle_2 \pm |V\rangle_1 |V\rangle_2] \otimes \frac{1}{\sqrt{2}} [|a\rangle_1 |b\rangle_2 \pm |b\rangle_1 |a\rangle_2], \quad (4)$$

$$|\Phi^\pm\rangle \otimes |\phi^\pm\rangle = \frac{1}{\sqrt{2}} [|H\rangle_1 |H\rangle_2 \pm |V\rangle_1 |V\rangle_2] \otimes \frac{1}{\sqrt{2}} [|a\rangle_1 |a\rangle_2 \pm |b\rangle_1 |b\rangle_2]. \quad (5)$$

## 2.1 General aspects of the WRHP

The Wigner transformation establishes a correspondence between a field operator acting on a vector in the Hilbert space and a (complex) amplitude of the field. In the context of PDC the electric field corresponding to a signal generated by the source (placed at  $\mathbf{r} = 0$ ) is represented by a slowly varying amplitude [12]:

$$\mathbf{F}_s^{(+)}(\mathbf{r}, t) = ie^{\omega_s t} \sum_{\mathbf{k} \in [\mathbf{k}]_s, \lambda=H,V} \left( \frac{\hbar \omega_{\mathbf{k}}}{2\epsilon_0 L^3} \right)^{\frac{1}{2}} \alpha_{\mathbf{k},\lambda}(t) \mathbf{u}_{\mathbf{k},\lambda} e^{i\mathbf{k} \cdot \mathbf{r}}, \quad (6)$$

where  $[\mathbf{k}]_s$  represents a set of wave vectors centered at  $\mathbf{k}_s$ , and  $\omega_s$  is the average frequency of the beam.  $\mathbf{u}_{\mathbf{k},\lambda}$  is a unit polarization vector. In the Heisenberg picture all the dynamics is contained at the amplitudes  $\alpha_{\mathbf{k},\lambda}(t)$ , while the Wigner function is time independent. In PDC the initial state is the vacuum, which is characterized by a electric field given by (6), by putting  $\alpha_{\mathbf{k},\lambda}(t) = \alpha_{\mathbf{k},\lambda} \exp(-i\omega_{\mathbf{k}} t)$ , where  $\alpha_{\mathbf{k},\lambda}$  represents the zeropoint amplitude corresponding to the mode  $\{\mathbf{k}, \lambda\}$ . The Wigner distribution for the vacuum field amplitudes is [11]:

$$W_{ZPF}(\{\alpha\}) = \prod_{[\mathbf{k}], \lambda} \frac{2}{\pi} e^{-2|\alpha_{\mathbf{k},\lambda}|^2}, \quad (7)$$

where  $\{\alpha\}$  represents the set of zeropoint amplitudes. Given two complex amplitudes,  $A(\mathbf{r}, t; \{\alpha\})$  and  $B(\mathbf{r}', t'; \{\alpha\})$ , the correlation between them is given by:

$$\langle AB \rangle \equiv \int W_{ZPF}(\{\alpha\}) A(\mathbf{r}, t; \{\alpha\}) B(\mathbf{r}', t'; \{\alpha\}) d\{\alpha\}. \quad (8)$$

For instance, from (7) the well known correlation properties hold:

$$\langle \alpha_{\mathbf{k}, \lambda} \alpha_{\mathbf{k}', \lambda'} \rangle = \langle \alpha_{\mathbf{k}, \lambda}^* \alpha_{\mathbf{k}', \lambda'}^* \rangle = 0 \quad ; \quad \langle \alpha_{\mathbf{k}, \lambda} \alpha_{\mathbf{k}', \lambda'}^* \rangle = \frac{1}{2} \delta_{\mathbf{k}, \mathbf{k}'} \delta_{\lambda, \lambda'}. \quad (9)$$

The single and joint detection probabilities in PDC experiments are calculated, in the Wigner approach, by means of the expressions [12]:

$$P_A \propto \langle I_A - I_{ZPF, A} \rangle \quad ; \quad P_{AB} \propto \langle (I_A - I_{ZPF, A})(I_B - I_{ZPF, B}) \rangle, \quad (10)$$

where  $I_i \propto \mathbf{F}_i^{(+)} \mathbf{F}_i^{(-)}$ ,  $i = A, B$ , is the intensity of light at the position of the i-detector, and  $I_{ZPF, i}$  is the corresponding intensity of the zeropoint field. In experiments involving polarization, the following simplified expression for the joint detection probability will be used for practical matters:

$$P_{AB}(\mathbf{r}, t; \mathbf{r}', t') \propto \sum_{\lambda} \sum_{\lambda'} \left| \left\langle F_{\lambda}^{(+)}(\phi_A; \mathbf{r}, t) F_{\lambda'}^{(+)}(\phi_B; \mathbf{r}', t') \right\rangle \right|^2, \quad (11)$$

where  $\phi_A$  and  $\phi_B$  are controllable parameters of the experimental setup.

## 2.2 WRHP description of polarization-momentum hyperentanglement

The study of polarization-momentum hyperentanglement in the WRHP is based on the same ideas that were developed in references [11] and [12]. The crucial point in the Wigner representation is that the selection of two sets of correlated beams,  $(a_1, b_2)$  and  $(a_2, b_1)$ , implies the consideration of eight sets of vacuum modes, which are “activated” and coupled with the laser inside the crystal (see fig.1). The set of representative modes corresponding to the entering zeropoint beam of wave vector  $\mathbf{k}_{a_i}$ , is represented by:

$$\{\alpha_{a_i, \lambda}\} \equiv \{\alpha_{\mathbf{k}, \lambda}; \mathbf{k} \in [\mathbf{k}]_{a_i}\} \quad ; \quad \lambda = H, V \quad ; \quad i = 1, 2. \quad (12)$$

In the same way, we have for  $\mathbf{k}_{b_i}$ :

$$\{\alpha_{b_i,\lambda}\} \equiv \{\alpha_{\mathbf{k},\lambda}; \mathbf{k} \in [\mathbf{k}]_{b_i}\} \quad ; \quad \lambda = H, V \quad ; \quad i = 1, 2. \quad (13)$$

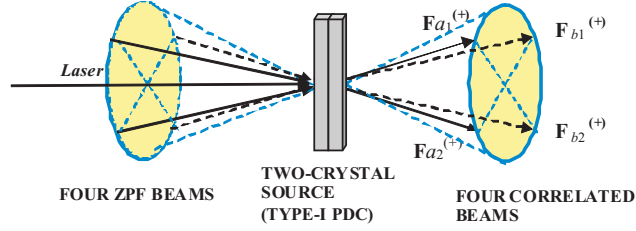


Figure 1: Sets of vacuum modes (on the left), which are “activated” and coupled with the laser inside the crystal. The correlation properties of the four beams (on the right) are related to the way in which the vacuum amplitudes are distributed in the field amplitudes.

In order to explain the main ideas of this subject we will first study one of the sixteen states, the one corresponding to Eq. (1). The hamiltonian corresponding to the electromagnetic field can be expressed in the following way:

$$H = H_{free} + H_{int} = \sum_{\lambda=H,V} \sum_{\mathbf{k}} \hbar \omega_{\mathbf{k},\lambda} \alpha_{\mathbf{k},\lambda}^* \alpha_{\mathbf{k},\lambda} + \left( i \hbar g' \frac{V}{2} \sum_{\substack{i,j=1 \\ i \neq j}}^2 \sum_{\lambda=H,V} \sum_{\substack{\mathbf{k} \in [\mathbf{k}]_{a_i} \\ \mathbf{k}' \in [\mathbf{k}]_{b_j}}} f(\mathbf{k}, \mathbf{k}') \exp(-i \omega_p t) \alpha_{\mathbf{k},\lambda}^* \alpha_{\mathbf{k}',\lambda}^* + \text{c.c.} \right), \quad (14)$$

where the crucial difference between (14) and Eq. (1) of [12] is that we have made the change  $V \rightarrow V/2$ , in order to consider that the energy of the

classical wave corresponding to the laser (with frequency  $\omega_p$  and momentum  $\mathbf{k}_p$ ), which is proportional to amplitude squared, must be divided into four beams. On the other hand,  $f(\mathbf{k}, \mathbf{k}')$  is a function which is different from zero only when the momentum matching condition is fulfilled, and  $g'$  is a constant related to the coupling parameter.

The evolution equation of  $\alpha_{\mathbf{k},\lambda}$  is given by the Hamilton (canonical) equations taking  $\sqrt{\hbar}\alpha_{\mathbf{k},\lambda}$  as coordinates, and  $\sqrt{\hbar}\alpha_{\mathbf{k},\lambda}^*$  as canonical momenta. We have:

$$\dot{\alpha}_{\mathbf{k},\lambda} = -i\omega_{\mathbf{k},\lambda}\alpha_{\mathbf{k},\lambda} + g'\frac{V}{2}\sum_{\mathbf{k}'}f(\mathbf{k}, \mathbf{k}')\exp(-i\omega_p t)\alpha_{\mathbf{k}',\lambda}^*, \quad (15)$$

where  $\{\mathbf{k}, \lambda\}$  represents any mode belonging to (12) or (13). The integration is performed to second order in the coupling constant ( $g = g'\Delta t$ ), from  $t = -\Delta t$  to  $t = 0$ ,  $\Delta t$  being the interaction time inside the two-crystal source (for more details see [11, 12]). In this way, for  $t > 0$  there is a free evolution, so that  $\alpha_{\mathbf{k},\lambda}(t) = \alpha_{\mathbf{k},\lambda}(0)\exp(-i\omega_{\mathbf{k}}t)$ ,  $\alpha_{\mathbf{k},\lambda}(0)$  being a linear transformation of the ZPF entering the crystal.

By substituting the amplitudes  $\alpha_{\mathbf{k},H}(t)$  and  $\alpha_{\mathbf{k},V}(t)$  in Eq. (6) we obtain the following four correlated beams leaving the crystal, which correspond to the description of the state  $|\Phi^+\rangle \otimes |\psi^+\rangle$ :  $\mathbf{F}_{a_1}^{(+)}$ ,  $\mathbf{F}_{b_2}^{(+)}$ ,  $\mathbf{F}_{b_1}^{(+)}$  and  $\mathbf{F}_{a_2}^{(+)}$ . The beam  $\mathbf{F}_{a_1}^{(+)}$  is correlated to  $\mathbf{F}_{b_2}^{(+)}$ , and  $\mathbf{F}_{b_1}^{(+)}$  is correlated to  $\mathbf{F}_{a_2}^{(+)}$ . For instance, the electric field corresponding to the beam  $\mathbf{F}_{a_1}^{(+)}$  is the sum of the zeropoint beam  $\mathbf{F}_{ZPF,a_1}^{(+)}$  (zeroth order term) plus a first order term resulting from the coupling between the laser beam and the zeropoint field corresponding to the conjugate direction  $\mathbf{F}_{ZPF,b_2}^{(-)}$ . Finally, the second order term modifies, to order  $g^2$ , the zeropoint amplitude  $\mathbf{F}_{ZPF,a_1}^{(+)}$ . We have:

$$\begin{aligned} \mathbf{F}_{a_1}^{(+)} &= \left(1 + \frac{g^2|V|^2}{4}J\right)\mathbf{F}_{ZPF,a_1}^{(+)} + \frac{gV}{2}G\mathbf{F}_{ZPF,b_2}^{(-)} \\ &= F_p^{(+)}(\mathbf{r}, t; \{\alpha_{a_1,H}; \alpha_{b_2,H}^*\})\mathbf{i}_{a_1} + F_s^{(+)}(\mathbf{r}, t; \{\alpha_{a_1,V}; \alpha_{b_2,V}^*\})\mathbf{j}_{a_1}, \end{aligned} \quad (16)$$

where  $G$  and  $J$  represent linear operators, and  $\mathbf{i}_{a_1}$  and  $\mathbf{j}_{a_1}$  are unit vectors representing horizontal and vertical linear polarization respectively. The field amplitudes  $F_p^{(+)}$  and  $F_s^{(+)}$  are defined by:

$$F_p^{(+)}(\mathbf{r}, t; \{\alpha_{a_1,H}; \alpha_{b_2,H}^*\}) = \left(1 + \frac{g^2|V|^2}{4}J\right)F_{ZPF,a_1,H}^{(+)} + \frac{gV}{2}GF_{ZPF,b_2,H}^{(-)},$$



$$F_s^{(+)}(\mathbf{r}, t; \{\alpha_{a_1, V}; \alpha_{b_2, V}^*\}) = (1 + \frac{g^2 |V|^2}{4} J) F_{ZPF_{a_1, V}}^{(+)} + \frac{gV}{2} G F_{ZPF_{b_2, V}}^{(-)}, \quad (17)$$

The same kind of description holds for the beams  $\mathbf{F}_{b_2}^{(+)}$ ,  $\mathbf{F}_{b_1}^{(+)}$  and  $\mathbf{F}_{a_2}^{(+)}$ , which can be presented in the following simplified form:

$$\mathbf{F}_{b_2}^{(+)}(\mathbf{r}, t) = F_q^{(+)}(\mathbf{r}, t; \{\alpha_{b_2, H}; \alpha_{a_1, H}^*\}) \mathbf{i}_{b_2} + F_r^{(+)}(\mathbf{r}, t; \{\alpha_{b_2, V}; \alpha_{a_1, V}^*\}) \mathbf{j}_{b_2}. \quad (18)$$

$$\mathbf{F}_{b_1}^{(+)}(\mathbf{r}, t) = F_p^{(+)}(\mathbf{r}, t; \{\alpha_{b_1, H}; \alpha_{a_2, H}^*\}) \mathbf{i}_{b_1} + F_s^{(+)}(\mathbf{r}, t; \{\alpha_{b_1, V}; \alpha_{a_2, V}^*\}) \mathbf{j}_{b_1}, \quad (19)$$

$$\mathbf{F}_{a_2}^{(+)}(\mathbf{r}, t) = F_q^{(+)}(\mathbf{r}, t; \{\alpha_{a_2, H}; \alpha_{b_1, H}^*\}) \mathbf{i}_{a_2} + F_r^{(+)}(\mathbf{r}, t; \{\alpha_{a_2, V}; \alpha_{b_1, V}^*\}) \mathbf{j}_{a_2}, \quad (20)$$

where we have included the sets of relevant zeropoint modes of each beam amplitude, as we have done in Eq. (16), for a better understanding of the correlation properties of the light beams. In this way,  $F_p^{(+)}$  is only correlated to  $F_q^{(+)}$  because  $\{\alpha_{a_1, H}\}$  is correlated to  $\{\alpha_{a_1, H}^*\}$ , and  $\{\alpha_{b_2, H}\}$  with  $\{\alpha_{b_2, H}^*\}$ , as it can be seen from Eq. (9). This reasoning applies also to  $F_r^{(+)}$  and  $F_s^{(+)}$ ,  $F_p^{(+)}$  and  $F_q^{(+)}$ , and  $F_r^{(+)}$  and  $F_s^{(+)}$ . All the rest crosscorrelations are null.

Taking  $\mathbf{r} = \mathbf{0}$  at the center of the source, we have:

$$\langle F_p^{(+)}(\mathbf{0}, t) F_q^{(+)}(\mathbf{0}, t') \rangle = g \frac{V}{2} \nu(t' - t), \quad (21)$$

where  $\nu(t' - t)$  is a function which vanishes when  $|t' - t|$  is greater than the correlation time between the beams  $\mathbf{F}_{a_1}^{(+)}$  and  $\mathbf{F}_{b_2}^{(+)}$  [13]. Similar expressions hold for  $\langle F_r^{(+)}(\mathbf{0}, t) F_s^{(+)}(\mathbf{0}, t') \rangle$ ,  $\langle F_p^{(+)}(\mathbf{0}, t) F_q^{(+)}(\mathbf{0}, t') \rangle$ , and  $\langle F_r^{(+)}(\mathbf{0}, t) F_s^{(+)}(\mathbf{0}, t') \rangle$ .

### 2.2.1 The sixteen hyper-Bell states in the WRHP

Let us now proceed to give a compact expression for the sixteen hyper-Bell states, for which purpose the description of the four polarization Bell-states in the WRHP, in terms of two-parametrized two correlated beams [16], will be considered here. For the sake of simplicity we shall discard in the rest of this section the dependence on position and time. For instance, the eight states  $|\Psi^\pm\rangle \otimes |\psi^\pm\rangle$  and  $|\Phi^\pm\rangle \otimes |\psi^\pm\rangle$  can be described in a compact form by the following four three-parametrized light beams:

$$\mathbf{F}_{a_1}^{(+)} = [F_s^{(+)} \cos \beta - F_p^{(+)} \sin \beta] \mathbf{i}_{a_1} + e^{i\kappa} [F_s^{(+)} \sin \beta + F_p^{(+)} \cos \beta] \mathbf{j}_{a_1}, \quad (22)$$

$$\mathbf{F}_{b_1}^{(+)} = \left[ [F_s'^{(+)} \cos \beta - F_p'^{(+)} \sin \beta] \mathbf{i}_{b_1} + e^{i\kappa} [F_s'^{(+)} \sin \beta + F_p'^{(+)} \cos \beta] \mathbf{j}_{b_1} \right] e^{i\varphi}, \quad (23)$$

$$\mathbf{F}_{a_2}^{(+)} = F_q'^{(+)} \mathbf{i}_{a_2} + F_r'^{(+)} \mathbf{j}_{a_2}, \quad (24)$$

$$\mathbf{F}_{b_2}^{(+)} = F_q^{(+)} \mathbf{i}_{b_2} + F_r^{(+)} \mathbf{j}_{b_2}, \quad (25)$$

where the combination  $\beta = 0, \kappa = 0$  ( $\beta = 0, \kappa = \pi$ ) corresponds to the description of the polarization state  $|\Psi^+\rangle$  ( $|\Psi^-\rangle$ ). In both cases the non null correlations correspond to different polarization components, the only difference being the minus sign that appears in the case of  $|\Psi^-\rangle$ . On the other hand, the case  $\beta = -\pi/2$  and  $\kappa = \pi$  ( $\beta = -\pi/2, \kappa = 0$ ) corresponds to the description of  $|\Phi^+\rangle$  ( $|\Phi^-\rangle$ ) where the horizontal (vertical) component of a beam is correlated with the horizontal (vertical) component of the other [16]. Finally, the parameter  $\varphi$  in equation (23) is related to the consideration of the momentum state  $|\psi^+\rangle$  (in the case  $\varphi = 0$ ) or  $|\psi^-\rangle$  (in the case  $\varphi = \pi$ ).

In order to change the momentum states  $|\psi^\pm\rangle$  to  $|\phi^\pm\rangle$ , we can consider the action of two polarizing beam-splitters in the paths  $a_1$  and  $b_1$  (or  $a_2$  and  $b_2$ ). For instance, PBS1 transmits vertical polarization and switches the momentum, and reflects horizontal polarization and the same mode remains. The second PBS2 operates in the opposite way.

The above considerations allow us to describe the sixteen hyper-Bell states in the WRHP by means of the following four six-parametrized correlated beams:

$$\mathbf{F}_{x_1}^{(+)} = [F_s^{(+)} \cos \beta - F_p^{(+)} \sin \beta] \mathbf{i}_{x_1} + e^{i\kappa} [F_s^{(+)} \sin \beta + F_p^{(+)} \cos \beta] \mathbf{j}_{x_1}, \quad (26)$$

$$\mathbf{F}_{y_1}^{(+)} = \left[ [F_s'^{(+)} \cos \beta - F_p'^{(+)} \sin \beta] \mathbf{i}_{y_1} + e^{i\kappa} [F_s'^{(+)} \sin \beta + F_p'^{(+)} \cos \beta] \mathbf{j}_{y_1} \right] e^{i\varphi_2}, \quad (27)$$

$$\mathbf{F}_{a_2}^{(+)} = F_q'^{(+)} \mathbf{i}_{a_2} + F_r'^{(+)} \mathbf{j}_{a_2}, \quad (28)$$

$$\mathbf{F}_{b_2}^{(+)} = F_q^{(+)} \mathbf{i}_{b_2} + F_r^{(+)} \mathbf{j}_{b_2}, \quad (29)$$

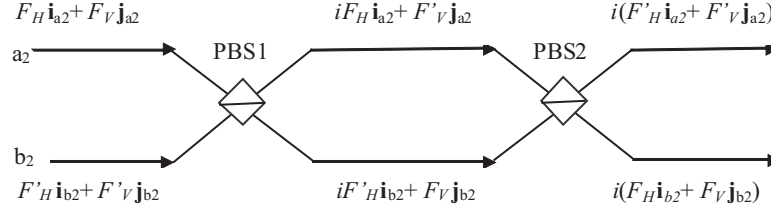


Figure 2: The action of two polarizing beam-splitters, operating in opposite ways, gives rise to a change in the momentum state, from  $|\psi^\pm\rangle$  to  $|\phi^\pm\rangle$ . In the Wigner representation, the complete operation is represented by the exchange  $F_H \longleftrightarrow F'_H$  and  $F_V \longleftrightarrow F'_V$ .

where the pair of parameters  $(x, y)$  can take the values  $(a, b)$  or  $(b, a)$ , and  $\mathbf{F}_{x_1}^{(+)}$  ( $\mathbf{F}_{y_1}^{(+)}$ ) is correlated to  $\mathbf{F}_{b_2}^{(+)}$  ( $\mathbf{F}_{a_2}^{(+)}$ ). Now, let us describe the different momentum states according to the values of  $x$ ,  $y$ ,  $\varphi_1$  and  $\varphi_2$ :

- The combination  $x \equiv a$ ,  $y \equiv b$ ,  $\varphi_1 = \varphi_2 = 0$  corresponds to the description of the states  $|\Psi^\pm\rangle \otimes |\psi^+\rangle$  and  $|\Phi^\pm\rangle \otimes |\psi^+\rangle$ .
- For  $x \equiv a$ ,  $y \equiv b$ ,  $\varphi_1 = 0$  and  $\varphi_2 = \pi$  we obtain the description of the states  $|\Psi^\pm\rangle \otimes |\psi^-\rangle$  and  $|\Phi^\pm\rangle \otimes |\psi^-\rangle$ .
- The values  $x \equiv b$ ,  $y \equiv a$ ,  $\varphi_1 = \varphi_2 = 0$ , correspond to the states  $|\Psi^\pm\rangle \otimes |\phi^+\rangle$  and  $|\Phi^\pm\rangle \otimes |\phi^+\rangle$ .
- Finally, in the case  $x \equiv b$ ,  $y \equiv a$ ,  $\varphi_1 = \pi$ , and  $\varphi_2 = 0$  we have  $|\Psi^\pm\rangle \otimes |\phi^-\rangle$  and  $|\Phi^\pm\rangle \otimes |\phi^-\rangle$ .

Eqs. (26) to (29) correspond to the description, in the WRHP, of the sixteen base Bell-states corresponding to polarization-momentum hyperentanglement of two photons. The essential point is that quantum correlations are

described in terms of four two by two correlated beams through the eight sets of independent zeropoint amplitudes entering the nonlinear source. Each of the sixteen states is defined by giving the values of six parameters:  $\beta$  and  $\kappa$  define the polarization Bell-state, and  $x$ ,  $y$ ,  $\varphi_1$  and  $\varphi_2$  the momentum Bell-state. These parameters can be changed locally, and this property is of interest in connection to dense coding and superdense coding [8, 9].

By comparing this analysis with the one corresponding to reference [16], we see that, in the case of polarization entanglement, only four independent sets of ZPF are needed at the source, and the four polarization Bell-states are described by means of two correlated beams, which are defined by giving the values of two parameters,  $\beta$  and  $\kappa$ .

### 3 COMPLETE BSM IN THE WRHP

In this section we shall apply the Wigner formalism developed in Sec. 2 to the description of a complete BSM of the four Bell states, by considering that one of the two degrees of freedom is in a fixed state: (i) First, we shall consider the experimental setup shown in Fig. 2 of reference [8], in which the momentum degrees of freedom are used as the ancilla, in order to encode information in polarization Bell states; (ii) in the second experiment (Fig. 3 of [8]), the polarization state is fixed, and the four momentum Bell-states can be distinguished. In both cases we shall describe the different steps of the experiments, in order to focus on the role of the zeropoint field.

The values of the field amplitudes at the detectors are usually computed by propagating them through the optical devices from the source to the detectors. In these experiments an identical distance separating the source from the respective optical devices and detectors will be considered, so that the contribution of the related phase shift in Eq. (16) of [12] will be discarded in the calculation of the probabilities. For simplicity we focus on the ideal situation  $t = t'$ , so that we can discard the dependence on position and time.

#### 3.1 Discrimination of the polarization Bell-states

The hyperentangled-Bell-state analyser includes two polarizing beam-splitters (PBS) which transmit (reflect) the vertical (horizontal) polarization, and switch modes (remain in the same mode), in order to perform a controlled-NOT (CNOT) logic operation between the polarization (control) and spacial

(target) degrees of freedom. Each outgoing beam passes through a polarization analyzer (PA) in the  $\pm 45^\circ$  basis, consisting of a half wave plate, a PBS, and two detectors. The vacuum zeropoint field at the idle channels of the analyzers is represented in Fig. 3.1, this being an important ingredient of our approach, as we shall see later.

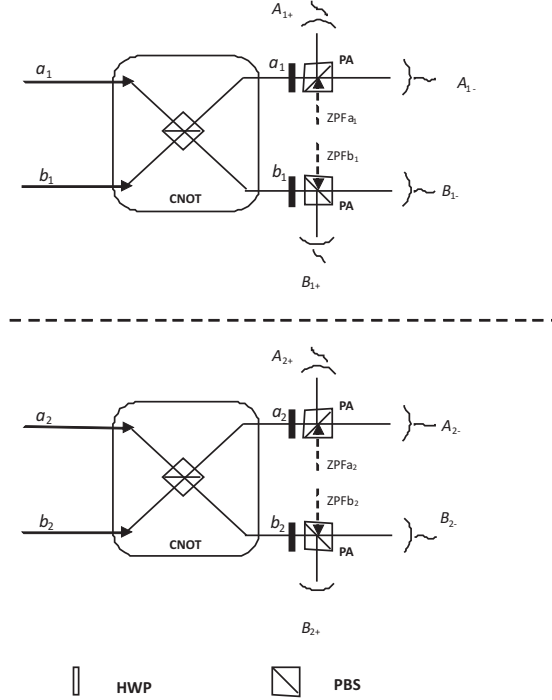


Figure 3: Polarization-momentum hyperentanglement analyzer. The consideration of the zeropoint field at the idle channels of the analyzers is a key point in the Wigner approach.

From equations (22) to (25), and by considering  $\varphi = 0$ , we obtain four correlated beams which describe one of the four states:  $|\Psi^\pm\rangle \otimes |\psi^+\rangle$  and  $|\Phi^\pm\rangle \otimes |\psi^+\rangle$ , depending on the value of  $\beta$  and  $\kappa$ . The action of CNOT gates is represented by the following output beams:

$$\mathbf{F}_{a_1}^{(+)} = i[F_s^{(+)} \cos \beta - F_p^{(+)} \sin \beta] \mathbf{j}_{a_1} + e^{i\kappa} [F_s^{(+)} \sin \beta + F_p^{(+)} \cos \beta] \mathbf{j}_{a_1}, \quad (30)$$

$$\mathbf{F}_{b_1}'^{(+)} = i[F_s'^{(+)}\cos\beta - F_p'^{(+)}\sin\beta]\mathbf{i}_{b_1} + e^{i\kappa}[F_s^{(+)}\sin\beta + F_p^{(+)}\cos\beta]\mathbf{j}_{b_1}, \quad (31)$$

$$\mathbf{F}_{a_2}'^{(+)} = iF_q'^{(+)}\mathbf{i}_{a_2} + F_r^{(+)}\mathbf{j}_{a_2}, \quad (32)$$

$$\mathbf{F}_{b_2}'^{(+)} = iF_q^{(+)}\mathbf{i}_{b_2} + F_r'^{(+)}\mathbf{j}_{b_2}, \quad (33)$$

where we have considered the imaginary unit in order to account for the reflection at the PBS, in contrast to the equation (3) of reference [8], in which there is no phase shift associated to the reflection.

A quick look at Eqs. (30) to (33) shows that, in the case  $\beta = 0$ , corresponding to the polarization states  $|\Psi^\pm\rangle$ , the nonzero correlations are those concerning amplitudes related to orthogonal polarizations of beams  $a_1$  and  $a_2$ , or  $b_1$  and  $b_2$ , while in the case  $\beta = -\pi/2$  (polarization states  $|\Phi^\pm\rangle$ ), there is no change in the correlation properties of the light beams respect to the equations (22) to (25) (by putting  $\varphi = 0$ ). This implies that the momentum state  $|\psi^+\rangle$  can be used to discriminate between the four polarization Bell states (see Eq. (4) of [8]). It is worthy of note that there is no additional zeropoint amplitudes entering the PBS's at the CNOT gates (see Fig. 3.1), so that the PBS's mark the momentum state due to the consideration of the eight sets of independent zeropoint modes at the two-crystal source, and their subsequent redistribution in the beam's amplitudes.

Now, the action of the half-wave plate -HWP@45°- gives rise to the following components  $\mathbf{i}$  and  $\mathbf{j}$  in the expression of the field for path  $a_1$ :

$$\begin{aligned} \mathbf{F}_{a_1}''^{(+)} &= \hat{M}_{HWP}\mathbf{F}_{a_1}'^{(+)} = \begin{pmatrix} 0 & 1 \\ 1 & 0 \end{pmatrix} \begin{pmatrix} i[F_s'^{(+)}\cos\beta - F_p'^{(+)}\sin\beta] \\ e^{i\kappa}[F_s'^{(+)}\sin\beta + F_p'^{(+)}\cos\beta] \end{pmatrix} \\ &= e^{i\kappa}[F_s'^{(+)}\sin\beta + F_p'^{(+)}\cos\beta]\mathbf{i}_{a_1} + i[F_s'^{(+)}\cos\beta - F_p'^{(+)}\sin\beta]\mathbf{j}_{a_1}, \end{aligned} \quad (34)$$

where  $\hat{M}_{HWP}$  is the matrix representing the half-wave plate. For the rest of the paths, using the same transformation, we have:

$$\mathbf{F}_{b_1}''^{(+)} = e^{i\kappa}[F_s^{(+)}\sin\beta + F_p^{(+)}\cos\beta]\mathbf{i}_{b_1} + i[F_s'^{(+)}\cos\beta - F_p'^{(+)}\sin\beta]\mathbf{j}_{b_1}, \quad (35)$$

$$\mathbf{F}_{a_2}''^{(+)} = F_r^{(+)}\mathbf{i}_{a_2} + iF_q'^{(+)}\mathbf{j}_{a_2}, \quad (36)$$

$$\mathbf{F}_{b_2}''^{(+)} = F_r'^{(+)}\mathbf{i}_{b_2} + iF_q^{(+)}\mathbf{j}_{b_2}. \quad (37)$$

Now, taking into account that the polarization analyzers are oriented at  $45^\circ$ , the polarizing beam splitters will reflect (transmit) the component of the field along the unit vector  $\mathbf{i}$  ( $\mathbf{j}$ ), which is oriented at  $+45^\circ$  ( $-45^\circ$ ) with respect to the horizontal direction. In order to express the field amplitudes at the detectors, we must add the corresponding zero-point component that enters through the free channel of each PBS. We have:

$$\mathbf{F}_{A_{1+}}^{(+)} = \frac{i}{\sqrt{2}} \left\{ i[F_s^{(+)} \cos \beta - F_p^{(+)} \sin \beta] + e^{i\kappa} [F_s'^{(+)} \sin \beta + F_p'^{(+)} \cos \beta] \right\} \mathbf{i} + [\mathbf{F}_{ZPFA_1}^{(+)} \cdot \mathbf{j}] \mathbf{j}, \quad (38)$$

$$\mathbf{F}_{A_{1-}}^{(+)} = \frac{1}{\sqrt{2}} \left\{ i[F_s^{(+)} \cos \beta - F_p^{(+)} \sin \beta] - e^{i\kappa} [F_s'^{(+)} \sin \beta + F_p'^{(+)} \cos \beta] \right\} \mathbf{j} + i[\mathbf{F}_{ZPFA_1}^{(+)} \cdot \mathbf{i}] \mathbf{i}, \quad (39)$$

$$\mathbf{F}_{B_{1+}}^{(+)} = \frac{i}{\sqrt{2}} \left\{ i[F_s'^{(+)} \cos \beta - F_p'^{(+)} \sin \beta] + e^{i\kappa} [F_s^{(+)} \sin \beta + F_p^{(+)} \cos \beta] \right\} \mathbf{i} + [\mathbf{F}_{ZPFB_1}^{(+)} \cdot \mathbf{j}] \mathbf{j}, \quad (40)$$

$$\mathbf{F}_{B_{1-}}^{(+)} = \frac{1}{\sqrt{2}} \left\{ i[F_s'^{(+)} \cos \beta - F_p'^{(+)} \sin \beta] - e^{i\kappa} [F_s^{(+)} \sin \beta + F_p^{(+)} \cos \beta] \right\} \mathbf{j} + i[\mathbf{F}_{ZPFB_1}^{(+)} \cdot \mathbf{i}] \mathbf{i}, \quad (41)$$

and for the paths  $a_2$  and  $b_2$

$$\mathbf{F}_{A_{2+}}^{(+)} = \frac{i}{\sqrt{2}} [iF_q'^{(+)} + F_r^{(+)}] \mathbf{i} + [\mathbf{F}_{ZPFA_2}^{(+)} \cdot \mathbf{j}] \mathbf{j}, \quad (42)$$

$$\mathbf{F}_{A_{2-}}^{(+)} = \frac{1}{\sqrt{2}} [iF_q'^{(+)} - F_r^{(+)}] \mathbf{j} + i[\mathbf{F}_{ZPFA_2}^{(+)} \cdot \mathbf{i}] \mathbf{i}, \quad (43)$$

$$\mathbf{F}_{B_{2+}}^{(+)} = \frac{i}{\sqrt{2}} [iF_q^{(+)} + F_r'^{(+)}] \mathbf{i} + [\mathbf{F}_{ZPFB_2}^{(+)} \cdot \mathbf{j}] \mathbf{j}, \quad (44)$$

$$\mathbf{F}_{B_{2-}}^{(+)} = \frac{1}{\sqrt{2}} [iF_q^{(+)} - F_r'^{(+)}] \mathbf{j} + i[\mathbf{F}_{ZPFB_2}^{(+)} \cdot \mathbf{i}] \mathbf{i}. \quad (45)$$

In order to calculate the joint detection probabilities we shall use Eq. (11) along with the correlation properties given in Eq. (21). We shall take into account that the ZPF inputs at the PBS's are uncorrelated with the signals and with each other. The crosscorrelations involved in Eq. (11) are expressed at the center of the source ( $\mathbf{r} = 0$ ), so that

$$|\langle F_p^{(+)}(\mathbf{0}, t) F_q^{(+)}(\mathbf{0}, t) \rangle|^2 = \frac{g^2 |V|^2 |\nu(0)|^2}{4}, \quad (46)$$

with similar expressions for  $|\langle F_r^{(+)} F_s^{(+)} \rangle|^2$ ,  $|\langle F_p'^{(+)} F_q'^{(+)} \rangle|^2$  and  $|\langle F_r'^{(+)} F_s'^{(+)} \rangle|^2$ .

- *Case I* ( $\beta = 0$ ) corresponds to the states  $|\Psi^\pm\rangle \otimes |\psi^+\rangle$ . After some easy calculations we obtain:

$$\frac{P_{A_{1+}, A_{2+}}}{k_{A_{1+}} k_{A_{2+}}} = \frac{P_{B_{1+}, B_{2+}}}{k_{B_{1+}} k_{B_{2+}}} = \frac{P_{A_{1-}, A_{2-}}}{k_{A_{1-}} k_{A_{2-}}} = \frac{P_{B_{1-}, B_{2-}}}{k_{B_{1-}} k_{B_{2-}}} = \frac{g^2 |V|^2 |\nu(0)|^2}{16} |1 + e^{i\kappa}|^2, \quad (47)$$

$$\frac{P_{A_{1+}, A_{2-}}}{k_{A_{1+}} k_{A_{2-}}} = \frac{P_{B_{1+}, B_{2-}}}{k_{B_{1+}} k_{B_{2-}}} = \frac{P_{A_{1-}, A_{2+}}}{k_{A_{1-}} k_{A_{2+}}} = \frac{P_{B_{1-}, B_{2+}}}{k_{B_{1-}} k_{B_{2+}}} = \frac{g^2 |V|^2 |\nu(0)|^2}{16} |1 - e^{i\kappa}|^2, \quad (48)$$

where  $k_{A_{1+}}$ ,  $k_{A_{1-}}$ ,  $k_{A_{2+}}$ ,  $k_{A_{2-}}$ ,  $k_{B_{1+}}$ ,  $k_{B_{1-}}$ ,  $k_{B_{2+}}$ ,  $k_{B_{2-}}$  are constants which are related to the effective efficiency of the detection process. From (47) and (48) it can be easily shown that for  $\kappa = 0$  ( $\kappa = \pi$ ), which corresponds to the polarization state  $|\Psi^+\rangle$  ( $|\Psi^-\rangle$ ), only the four probabilities concerning the same orientation (different orientation) of the output ports are different from zero, so that the detector signatures will allow to distinguish between these two states.

- *Case II* ( $\beta = -\pi/2$ ) corresponds to the states  $|\Phi^\pm\rangle \otimes |\psi^+\rangle$ . After some easy calculations we obtain:

$$\frac{P_{A_{1+}, B_{2+}}}{k_{A_{1+}} k_{B_{2+}}} = \frac{P_{B_{1+}, A_{2+}}}{k_{B_{1+}} k_{A_{2+}}} = \frac{P_{A_{1-}, B_{2-}}}{k_{A_{1-}} k_{B_{2-}}} = \frac{P_{B_{1-}, A_{2-}}}{k_{B_{1-}} k_{A_{2-}}} = \frac{g^2 |V|^2 |\nu(0)|^2}{16} |i^2 - e^{i\kappa}|^2, \quad (49)$$

$$\frac{P_{A_{1+}, B_{2-}}}{k_{A_{1+}} k_{B_{2-}}} = \frac{P_{B_{1+}, A_{2-}}}{k_{B_{1+}} k_{A_{2-}}} = \frac{P_{A_{1-}, B_{2+}}}{k_{A_{1-}} k_{B_{2+}}} = \frac{P_{B_{1-}, A_{2+}}}{k_{B_{1-}} k_{A_{2+}}} = \frac{g^2 |V|^2 |\nu(0)|^2}{16} |i^2 + e^{i\kappa}|^2, \quad (50)$$

In this case, from (49) and (50) it is shown that for  $\kappa = 0$  ( $\kappa = \pi$ ), which corresponds to the polarization state  $|\Phi^-\rangle$  ( $|\Phi^+\rangle$ ), only the four probabilities concerning the same orientation (different orientation) of the output ports are different from zero, so that the detector signatures will allow us to distinguish between these two states.



The discrepancy with Walborn's Table I in ref. [8], with respect to the states  $|\Phi^-\rangle$  and  $|\Phi^+\rangle$ , is due to the consideration of the complex factor  $i$  for the reflected amplitudes at the CNOT gates [18]. For this reason, the corresponding joint probabilities for these two states are exchanged with respect to the work of Walborn et al.

### 3.2 Discrimination of the momentum Bell-states

The experimental setup is shown in Fig. 3.2. Two half-wave plates (HWP), which are aligned at  $45^\circ$  in modes  $b_1$  and  $b_2$ , perform the CNOT operation. The  $BS$  are balanced nonpolarizing beam splitters [8]. In this case, the polarization degrees of freedom are used as ancilla, so that the polarization state is fixed, and corresponds to  $|\Psi^+\rangle$ . In the Wigner formalism, by putting  $\kappa = \beta = 0$  in Eqs. (26) to (29), we obtain the following four beams in order to compactly describe the four states  $|\Psi^+\rangle \otimes |\psi^\pm\rangle$  and  $|\Psi^+\rangle \otimes |\phi^\pm\rangle$ :

$$\mathbf{F}_{x_1}^{(+)} = [F_s^{(+)}\mathbf{i}_{x_1} + F_p^{(+)}\mathbf{j}_{x_1}]e^{i\varphi_1}, \quad (51)$$

$$\mathbf{F}_{y_1}^{(+)} = [F'_s{}^{(+)}\mathbf{i}_{y_1} + F'_p{}^{(+)}\mathbf{j}_{y_1}]e^{i\varphi_2}, \quad (52)$$

$$\mathbf{F}_{a_2}^{(+)} = F'_q{}^{(+)}\mathbf{i}_{a_2} + F'_r{}^{(+)}\mathbf{j}_{a_2}, \quad (53)$$

$$\mathbf{F}_{b_2}^{(+)} = F_q^{(+)}\mathbf{i}_{b_2} + F_r^{(+)}\mathbf{j}_{b_2}. \quad (54)$$

In order to consider all the possibilities in our calculation, we shall define the matrices  $\hat{M}_x$  and  $\hat{M}_y$ : in the case  $x = a$ ,  $y = b$ ,  $\hat{M}_x = \hat{I}$  (identity matrix) and  $\hat{M}_y = \hat{M}_{HWP}$ ; on the other hand, if  $x = b$ ,  $y = a$ , then  $\hat{M}_x = \hat{M}_{HWP}$  and  $\hat{M}_y = \hat{I}$ . We have:

$$\mathbf{F}_{x_1}^{(+)} = \hat{M}_x \mathbf{F}_{x_1}^{(+)} = e^{i\varphi_1} \left\{ [m_{x11}F_s^{(+)} + m_{x12}F_p^{(+)}]\mathbf{i}_{x_1} + [m_{x21}F_s^{(+)} + m_{x22}F_p^{(+)}]\mathbf{j}_{x_1} \right\}, \quad (55)$$

where  $m_{x_{ij}} = \delta_{ij}$  ( $m_{x_{ij}} = 1 - \delta_{ij}$ ) in the case  $x = a$  ( $x = b$ ).

$$\mathbf{F}'_{y_1}{}^{(+)} = \hat{M}_y \mathbf{F}'_{y_1}{}^{(+)} = e^{i\varphi_2} \left\{ [m_{y11}F'_s{}^{(+)} + m_{y12}F'_p{}^{(+)}]\mathbf{i}_{y_1} + [m_{y21}F'_s{}^{(+)} + m_{y22}F'_p{}^{(+)}]\mathbf{j}_{y_1} \right\}, \quad (56)$$

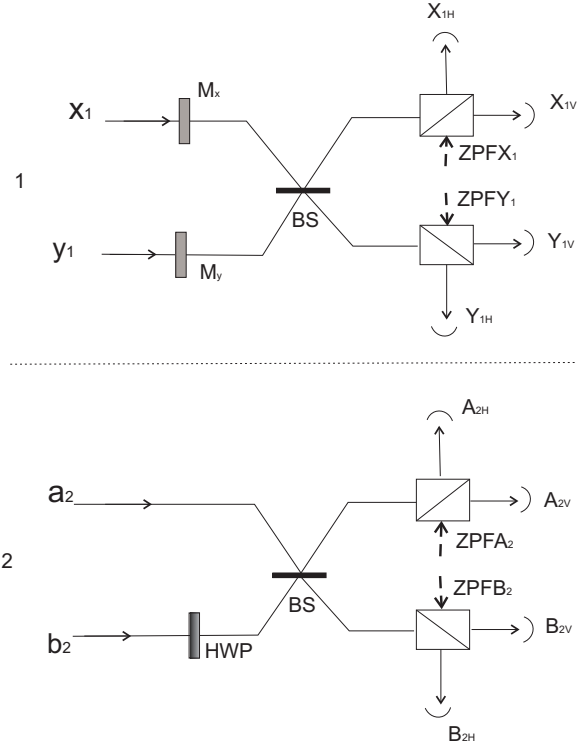


Figure 4: Hyperentangled-Bell-state analyzer using a fixed entangled state in polarization. We have represented two optical devices,  $M_x$  and  $M_y$ , in order to account for the two possibilities, depending on the value of  $x$  and  $y$ . The zeropoint field at the idle channels of the analyzers is represented by four beams.

where  $m_{y_{ij}} = \delta_{ij}$  ( $m_{y_{ij}} = 1 - \delta_{ij}$ ) in the case  $y = a$  ( $y = b$ ).

$$\mathbf{F}_{a_2}'^{(+)} = \mathbf{F}_{a_2}^{(+)} = F_q^{(+)} \mathbf{i}_{a_2} + F_r^{(+)} \mathbf{j}_{a_2}, \quad (57)$$

$$\mathbf{F}_{b_2}'^{(+)} = \hat{M}_{HWP} \mathbf{F}_{b_2}^{(+)} = F_r^{(+)} \mathbf{i}_{b_2} + F_q^{(+)} \mathbf{j}_{b_2}. \quad (58)$$

From Eqs. (55) to (58) it can be easily seen that, for  $x = a$ ,  $y = b$  ( $x = b$ ,  $y = a$ ), the only non null crosscorrelations are those concerning the same polarization (orthogonal polarizations). For this reason, the CNOT operation marks the polarization state. This operation does not introduce additional zeropoint fluctuations, because the HWP's do not activate zeropoint modes.

The beam splitters transform the input beams as  $\mathbf{F}_{x_1}'^{(+)} \rightarrow (1/\sqrt{2})[i^{n_1} \mathbf{F}_{x_1}'^{(+)} + \mathbf{F}_{y_1}'^{(+)}]$ ,  $\mathbf{F}_{y_1}'^{(+)} \rightarrow (1/\sqrt{2})[\mathbf{F}_{x_1}'^{(+)} + i^{n_2} \mathbf{F}_{y_1}'^{(+)}]$ , where the values of  $n_1$  and  $n_2$  depend on the kind of *BS*. We shall consider two possibilities: (i)  $n_1 = n_2 = 1$ , i.e. the reflected amplitude contains an imaginary unit; (ii)  $n_1 = 0$  and  $n_2 = 2$  ( $n_1 = 2$  and  $n_2 = 0$ ) in the case  $x = a$ ,  $y = b$  ( $x = b$ ,  $y = a$ ), this corresponding to a beam-splitter that performs the Hadamard transformation. In the same way,  $\mathbf{F}_{a_2}'^{(+)} \rightarrow (1/\sqrt{2})[i^{n'_1} \mathbf{F}_{a_2}'^{(+)} + \mathbf{F}_{b_2}'^{(+)}]$ ,  $\mathbf{F}_{b_2}'^{(+)} \rightarrow (1/\sqrt{2})[\mathbf{F}_{a_2}'^{(+)} + i^{n'_2} \mathbf{F}_{b_2}'^{(+)}]$ , where  $n'_1 = n'_2 = 1$  take the same values as in the cases (i) and (ii). This operation does not introduce any additional zeropoint amplitudes because there is no idle channel at the BS's.

Finally, if we consider the zeropoint amplitudes at the idle channels of the PBS's (see Fig. 3.2), the field amplitudes at the detectors are:

$$F_{X_{1H}}^{(+)} = \frac{i}{\sqrt{2}} \left\{ i^{n_1} e^{i\varphi_1} [m_{x_{11}} F_s^{(+)} + m_{x_{12}} F_p^{(+)}] + e^{i\varphi_2} [m_{y_{11}} F_s^{(+)} + m_{y_{12}} F_p^{(+)}] \right\} + F_{vac, X_{1H}}^{(+)}, \quad (59)$$

$$F_{X_{1V}}^{(+)} = \frac{1}{\sqrt{2}} \left\{ i^{n_1} e^{i\varphi_1} [m_{x_{21}} F_s^{(+)} + m_{x_{22}} F_p^{(+)}] + e^{i\varphi_2} [m_{y_{21}} F_s^{(+)} + m_{y_{22}} F_p^{(+)}] \right\} + F_{vac, X_{1V}}^{(+)}, \quad (60)$$

$$F_{Y_{1H}}^{(+)} = \frac{i}{\sqrt{2}} \left\{ e^{i\varphi_1} [m_{x_{11}} F_s^{(+)} + m_{x_{12}} F_p^{(+)}] + i^{n_2} e^{i\varphi_2} [m_{y_{11}} F_s^{(+)} + m_{y_{12}} F_p^{(+)}] \right\} + F_{vac, Y_{1H}}^{(+)}, \quad (61)$$

$$F_{Y_{1V}}^{(+)} = \frac{1}{\sqrt{2}} \left\{ e^{i\varphi_1} [m_{x_{21}} F_s^{(+)} + m_{x_{22}} F_p^{(+)}] + i^{n_2} e^{i\varphi_2} [m_{y_{21}} F_s^{(+)} + m_{y_{22}} F_p^{(+)}] \right\} + F_{vac, Y_{1V}}^{(+)}, \quad (62)$$

$$F_{A_{2H}}^{(+)} = \frac{i}{\sqrt{2}}[i^{n'_1} F_q^{(+)} + F_r^{(+)}] + F_{vac, A_{2H}}^{(+)}, \quad (63)$$

$$F_{A_{2V}}^{(+)} = \frac{1}{\sqrt{2}}[i^{n'_1} F_r^{(+)} + F_q^{(+)}] + F_{vac, A_{2V}}^{(+)}, \quad (64)$$

$$F_{B_{2H}}^{(+)} = \frac{i}{\sqrt{2}}[F_q^{(+)} + i^{n'_2} F_r^{(+)}] + F_{vac, B_{2H}}^{(+)}, \quad (65)$$

$$F_{B_{2V}}^{(+)} = \frac{1}{\sqrt{2}}[F_r^{(+)} + i^{n'_2} F_q^{(+)}] + F_{vac, B_{2V}}^{(+)}. \quad (66)$$

Now, using Eqs. (21) and (11), and taking into account that the ZPF inputs at the PBS's are uncorrelated with the signals and with each other, we shall consider the following cases:

- *Case I* ( $x = a, y = b$ ) corresponds to the states  $|\Psi^+\rangle \otimes |\psi^\pm\rangle$ . After some easy algebra, we obtain:

$$\frac{P_{A_{1H}, A_{2H}}}{k_{A_{1H}} k_{A_{2H}}} = \frac{P_{B_{1H}, B_{2H}}}{k_{B_{1H}} k_{B_{2H}}} = \frac{P_{A_{1V}, A_{2V}}}{k_{A_{1V}} k_{A_{2V}}} = \frac{P_{B_{1V}, B_{2V}}}{k_{B_{1V}} k_{B_{2V}}} = \frac{g^2 |V|^2 |\nu(0)|^2}{16} |e^{i\varphi_1} + e^{i\varphi_2}|^2, \quad (67)$$

and

$$\frac{P_{A_{1H}, B_{2H}}}{k_{A_{1H}} k_{B_{2H}}} = \frac{P_{B_{1H}, A_{2H}}}{k_{B_{1H}} k_{A_{2H}}} = \frac{P_{A_{1V}, B_{2V}}}{k_{A_{1V}} k_{B_{2V}}} = \frac{P_{B_{1V}, A_{2V}}}{k_{B_{1V}} k_{A_{2V}}} = \frac{g^2 |V|^2 |\nu(0)|^2}{16} |e^{i\varphi_1} - e^{i\varphi_2}|^2, \quad (68)$$

independently of the kind of beam-splitter used in the experiment, and described earlier.

From Eqs. (67) and (68) it can be seen that, in the case  $\varphi_1 = \varphi_2 = 0$  ( $\varphi_1 = 0, \varphi_2 = \pi$ ), which corresponds to the momentum state  $|\psi^+\rangle$  ( $|\psi^-\rangle$ ), only the four probabilities in Eq. (67) (Eq. (68)) are different from zero, so that the detector signatures will allow us to distinguish between these two states.

- *Case II* ( $x = b, y = a$ ) corresponds to the states  $|\Psi^+\rangle \otimes |\phi^\pm\rangle$ . In this case, we obtain:

$$\frac{P_{A_{1H}, A_{2V}}}{k_{A_{1H}} k_{A_{2V}}} = \frac{P_{A_{1V}, A_{2H}}}{k_{A_{1V}} k_{A_{2H}}} = \frac{g^2 |V|^2 |\nu(0)|^2}{16} |e^{i\varphi_1} + i^{n_2+n'_1} e^{i\varphi_2}|^2, \quad (69)$$

$$\frac{P_{B_{1H}, B_{2V}}}{k_{B_{1H}} k_{B_{2V}}} = \frac{P_{B_{1V}, B_{2H}}}{k_{B_{1V}} k_{B_{2H}}} = \frac{g^2 |V|^2 |\nu(0)|^2}{16} \left| e^{i\varphi_1} + i^{n_1+n'_2} e^{i\varphi_2} \right|^2, \quad (70)$$

In the situation corresponding to  $n_1 = n_2 = n'_1 = n'_2 = 1$ , the above probabilities are non null only in the case  $\varphi_1 = \pi$ ,  $\varphi_2 = 0$  (or viceversa), i.e. the WRHP description of the momentum state  $|\phi^-\rangle$ . In contrast, in the case of reference [8], in which  $n_1 = 2$ ,  $n_2 = 0$ ,  $n'_1 = 0$ ,  $n'_2 = 2$ , the expressions (69) and (70) are different from zero only when  $\varphi_1 = \varphi_2 = 0$ , i.e. the situation corresponding to the state  $|\phi^+\rangle$ .

On the other hand:

$$\frac{P_{A_{1H}, B_{2V}}}{k_{A_{1H}} k_{B_{2V}}} = \frac{P_{A_{1V}, B_{2H}}}{k_{A_{1V}} k_{B_{2H}}} = \frac{g^2 |V|^2 |\nu(0)|^2}{16} \left| i^{n'_1} e^{i\varphi_1} + i^{n_2} e^{i\varphi_2} \right|^2, \quad (71)$$

$$\frac{P_{B_{1H}, A_{2V}}}{k_{B_{1H}} k_{A_{2V}}} = \frac{P_{B_{1V}, A_{2H}}}{k_{B_{1V}} k_{A_{2H}}} = \frac{g^2 |V|^2 |\nu(0)|^2}{16} \left| i^{n_1} e^{i\varphi_1} + i^{n'_1} e^{i\varphi_2} \right|^2. \quad (72)$$

From Eqs. (71) and (72), if  $n_1 = n_2 = n'_1 = n'_2 = 1$  the corresponding probabilities are non null only in the case  $\varphi_1 = \varphi_2 = 0$ , i.e. the situation corresponding to the momentum state  $|\phi^+\rangle$ . Nevertheless, in the case of reference [8], in which  $n_1 = 2$ ,  $n_2 = 0$ ,  $n'_1 = 0$ ,  $n'_2 = 2$ , the expressions (71) and (72) are different from zero only when  $\varphi_1 = \pi$ ,  $\varphi_2 = 0$  (or viceversa), i.e. the situation corresponding to the state  $|\phi^-\rangle$ .

## 4 DISCUSSION AND CONCLUSIONS

We have applied the Wigner approach in the Heisenberg picture (WRHP) to study polarization-momentum hyperentanglement generated in parametric down-conversion. Also, we have analyzed two experimental setups for complete BSM, each using a fixed state in one of the two degrees of freedom, so that the information is encoded in the other, as it appears in reference [8]. As we have already pointed out, once within the Wigner framework, the typical quantum results appear precisely as a consequence of the role of the zeropoint field in the production, propagation, and detection of light. Quantum correlations can then be explained solely in terms of the propagation of those vacuum amplitudes through the experimental setup, and their subsequent subtraction at the detectors. Hence, the Wigner formalism allows for an interpretation of these experiments in terms of waves, where photons

are just wave-packets carrying the zeropoint amplitudes through the experimental setup, and finally detected. However, the whole formalism lies within the quantum domain, with the zero-point field as an equivalent to vacuum fluctuations in the Hilbert space.

The use of Hilbert spaces of higher dimensions is related, within the WRHP approach, to the inclusion of more sets of vacuum modes entering the crystal. With an increasing number of vacuum inputs, the possibility for extracting more information from the zeropoint field also increases. The crucial point concerning the generation of polarization-momentum hyperentanglement is the consideration of eight independent (uncorrelated) sets of vacuum modes, which are “activated” throughout a coupling with the laser inside the two-crystal source. In Ref. [16] it was stressed that two-photon entanglement in only one degree of freedom implies the consideration of four sets of zeropoint modes at the source. Hence we conjecture that, for a two-photon  $n$ -qubit state, the number of independent sets of zeropoint modes which are necessary for the generation of entanglement, is just  $2^{n+1}$ .

On the other hand, given an optical  $n$ -qubit state, the maximal number of mutually distinguishable sets of Bell states is above by  $2^{n+1}$  [9]. In this paper we have shown that, for  $n = 2$ , this number is exactly the same as the number of independent sets entering the source (the conclusion holds in the case  $n = 1$ ). Then, we can conjecture that, for a given  $n$ , the maximal distinguishability in a Bell-like experiment is bounded by the number of independent vacuum sets of modes which are extracted at the source. In other words, the number of relevant sets of zeropoint modes at the source represents a limit on optimal Bell-state analysis in the enlarged Hilbert space.

Eqs. (26) to (29) give the WRHP description of the sixteen Bell-like states in terms of four two by two correlated beams. Each of the states is described by giving the value of six parameters: two of them ( $\beta$  and  $\kappa$ ) indicate the polarization Bell-state, and the other four ( $x$ ,  $y$ ,  $\varphi_1$  and  $\varphi_2$ ) are related to the momentum. Let us emphasize that these parameters can be locally controlled because all of them appear in Eqs. (26) and (27), corresponding to the photon 1. Hence dense coding [8] and superdense coding [9] are justified, in the context of WRHP, by the possibility of changing the correlation properties of the four beams through the action of a linear optical device which operates in the same way as in classical optics. This contrasts with the usual description in the Hilbert space, in which local operations are represented by unitary operators. In the Wigner framework, the effect of a linear optical device on a beam accounts for a change in the

distribution of the zeropoint amplitudes inside the field components, so that there is a change in the correlation properties. Because these operations do not introduce additional zeropoint noise, the information encoded in the zeropoint amplitudes entering the source can be manipulated in order to complete successfully a quantum dense coding protocol.

Moreover, the noise entering the idle channels of the analyzers limits the optimality of the Bell-state analysis, and this idea is worthy of consideration. For instance, in Section 3 we have applied the WRHP formalism to complete BSM, in the case where one of the degrees of freedom is in a fixed (ancillary) state, and the information is encoded at the other degree of freedom. In Walborn's experiments, we see that eight sets of ZPF modes enter the source but the analyzer has four idle channels, i.e. four entry points for noise. Hence, we can determine the number of Bell states that can be distinguished by subtracting the number of channels with noise from the number of ZPF entry modes, so that in this case we have  $8 - 4 = 4$ . The same reasoning applies to the partial Bell-state analysis described in [16]: if we consider the four independent sets of vacuum amplitudes at the source, and two idle channels at the Bell-state analyzer (see Fig. 1 of reference [16]), the difference  $4 - 2 = 2$  just gives the maximum number of polarization Bell-states that can be distinguished using linear optics and single photon detectors.

The main conclusion of this work is that the WRHP approach allows for the possibility of obtaining additional information to the one provided by the standard Hilbert space formalism, just by considering the role of the zeropoint field at the different steps of an optical quantum communication experiment using PDC. We conjecture that there is a close relationship between the zeropoint extracted at the source, the corresponding zeropoint field entering the vacuum channels of the analyzers, and the maximal information that can be extracted in a concrete experiment. This idea will be developed in further works.

## 5 ACKNOWLEDGEMENTS

The authors would like to thank Prof. E. Santos for revising the manuscript, and for helpful suggestions and comments on the work. A. Casado acknowledge the support from the Spanish MCI Project no. FIS2011-29400.

## References

- [1] N. Gisin, G. Ribordy, W. Tittel, and H. Zbinden, *Rev. Mod. Phys.* **74**, 145 (2002)
- [2] C. H. Bennett and S. J. Wiesner, *Phys. Rev. Lett.* **69**, 2881 (1992).
- [3] D. Bouwmeester, J. W. Pan, K. Mattle, M. Eibl, H. Weinfurter, and A. Zeilinger, *Nature* **390**, 675 (1997); D. Boschi, S. Branca, F. De Martini, L. Hardy, and S. Popescu, *Phys. Rev. Lett.* **80**, 1121 (1998).
- [4] K. Mattle, H. Weinfurter, P. G. Kwiat, and A. Zeilinger, *Phys. Rev. Lett.* **76**, 4656 (1996).
- [5] P. G. Kwiat and H. Weinfurter, *Phys. Rev. A* **58**, R2623 (1998).
- [6] G. Vallone, E. Pomarico, P. Mataloni, F. De Martini, and V. Berardi, *Physical Review Letters* **98**, 180502 (2007).
- [7] M. S. Tame, R. Prevede, M. Paternostro, P. Bhi, M. S. Kim, and A. Zeilinger, *Phys. Rev. Lett.* **98**, 140501 (2007).
- [8] S. P. Walborn, S. Pádua, and C. H. Monken, *Phys. Rev. A* **68**, 042313 (2003).
- [9] T.-C. Wei, J. T. Barreiro, and P. G. Kwiat, *Phys. Rev. A* **75**, 060305(R) (2007).
- [10] N. Pienti, C. P. E. Gaebler, and T. W. Lynn, *Phys. Rev. A* **84**, 022340 (2011).
- [11] A. Casado, A. Fernández-Rueda, T. W. Marshall, R. Risco-Delgado, and E. Santos, *Phys. Rev. A* **55**, 3879 (1997).
- [12] A. Casado, T. W. Marshall, and E. Santos, *J. Opt. Soc. Am. B* **15**, 1572 (1998).
- [13] A. Casado, A. Fernández-Rueda, T. W. Marshall, J. Martínez, R. Risco-Delgado, and E. Santos, *Eur. Phys. J. D* **11**, 465 (2000).
- [14] A. Casado, T. W. Marshall, R. Risco-Delgado, and E. Santos, *Eur. Phys. J. D* **13**, 109 (2001).



- [15] A. Casado, S. Guerra, and J. Plácido, *J. Phys. B: At. Mol. Opt. Phys.* **41**, 045501 (2008).
- [16] A. Casado, S. Guerra, and J. Plácido, *Advances in Mathematical Physics* **Volume 2010**, Article ID 501521, 11 pages doi:10.1155/2010/501521 (2010).
- [17] P. G. Kwiat, E. Waks, A. G. White, I. Appelbaum, and P. H. Eberhard, *Phys. Rev. A* **60**, R773 (1999).
- [18] A. Zeilinger, *Am. J. Phys.* **49** 9, 882 (1981).